

NEW ACCELERATING SECTIONS FOR THE 2 GeV LINAC
E.Z. Biller, V.A. Vishnyakov and A.N. Dovbnya
Kharkov Institute of Physics and Technology,
The Ukrainian Academy of Sciences
310108 Kharkov, USSR

Abstract

New accelerating sections have been designed and constructed to increase the beam energy in the 2 GeV electron linac. This report describes the choice of the accelerating structure, the results of the computations and tests. The average accelerating gradient obtained is above 20 MeV/m for a 4.3-m section length.

The Kharkov electron linac was brought into service in 1965. During 20 years of its operation 10^5 man-hours have been devoted to physics research. At present the linac has a peak energy of 1.8 GeV and a peak current limited to 100 mA due to the beam breakup resulting from the beam-EH_{II}-wave interaction. The beam intensity was increased by suppressing the EH_{II}-wave with radial slits cut in the waveguide disks in 20 sections and improving the beam focusing system and the field symmetry in the couplers.

The use of the linac as an injector for a stretcher¹⁾ requires a factor of 2 greater energy which we intend to obtain by installing new accelerating sections and increasing the RF power.

Choice of the Accelerating Structure

The injected beam current pulse width of 1.4 μ s and the RF pulse of 2.5 μ s delivered by a klystron, set the following limits on the choice of the accelerating structure:

- (i) the section length cannot be changed (4.3 m),
- (ii) the filling time of each section should not exceed 1 μ s,
- (iii) at the first stage 20 MW klystrons and at the second stage 40 MW klystrons would be employed; the latter may be combined with cavities (like in SLED²⁾), and
- (iv) the average accelerating gradient at

the first stage should be 15 MeV/m and at the second stage 22 to 30 MeV/m.

Considering the above limitations, we analyzed a number of prototype accelerating sections which might be more promising as regards the accelerating gradient. The analysis led us to conclude:

- a) standing-wave structures are not useful since they have a lower accelerating gradient for a section length greater than 4 m and are highly frequency-sensitive,
- b) structures with low damping and a high group velocity currently developed at many laboratories do not give a higher accelerating gradient with a beam current in excess of 0.1 A,
- c) it does not seem worth-while to install a series of shorter-length accelerating sections along the given circumference of the linac, simultaneously providing a parallel RF power supply to the sections from a single klystron, and
- d) to increase the energy one has to employ a disk-loaded waveguide with a quasi-constant field gradient.

In fig.1 the energy gain and the filling time are plotted versus the field load (a/λ) for the constant-impedance structure. Also shown are the data obtained for two shorter-length sections with individual parallel power supply. It can be seen that the use of shorter sections is not beneficial even though the current loading is taken into account. With the current equal to 0.1...0.2 A, the energy dependence peak corresponds to the filling time of 1 μ s. Fig.2 compares the energy gain dependence on the filling time for a 4.3-m section in a disk-loaded- and a linear collider structures.³⁾ The latter has a smaller filling time therefore an alternative version of a "longer section" was considered where the power from several sources is integrated. The application of

of this structure gives practically no appreciable energy gain either and entails great difficulties.

A section with a quasi-constant accelerating gradient operates in the $\pi/2$ mode of oscillations at 2 797.000 MHz. The choice of the oscillation mode is due to the electric strength of the resonator (here the surface field and the stored energy were measured to be by 15% smaller than for the $2/3 \pi$ -mode) and easy post-manufacture tuning of the section. To suppress the beam breakup along the axis of the linac it is intended to fabricate 5 types of accelerating section detuned in $\text{EH}_{\text{II}}(0, \pm 2, \pm 4 \text{ MHz})$. In the loading disks in the first 10 sections cross-like slits will be made. The table below lists the geometric characteristics of the basic type of accelerating section.

Table: Cavity Parameters for a Basic Section

Parameter	Subsection			
	1	2	3	4
Waveguide inside diameter (mm)	84.812	84.382	83.926	83.961
Disk thickness (mm)	4.072	4.072	4.072	4.072
Disk hole diameter (mm)	25.444	23.627	21.821	19.613
Ring circumference (mm)	22.722	22.722	22.722	22.722
Filling time (μs)	0.150	0.191	0.248	0.353
Damping constant	0.122	0.1658	0.213	0.385
Field loading	0.1187	0.1100	0.1020	0.0915
Group velocity	0.0239	0.0187	0.0144	0.0101

Prototype Section

To check the technique of fabrication adopted and simulate the operation at the input RF power of 40 MW, a 4.3-m section with a constant impedance was constructed and tested. The field loading was chosen to be 0.1020 corresponding to the operating conditions of the third subsection. The filling time was 0.94 μs . At the beginning of the section it was possible to obtain an average field strength up to 21 MeV/m at the input RF power approaching 20 MW, which would correspond to the quasi-constant gradient operation at the input RF power of 40 MW. The cavities were assembled from annular disks and cylinders with bores used to cool the section.⁴⁾ The tuning of the cavities in the range of

$\pm 40 \text{ kHz}$ was performed by varying the inside diameter of the cylinders. The cavities were brazed with a silver alloy in vacuum. The $\pi/2$ couplers were employed where the field symmetry was achieved by means of an evanescent waveguide placed opposite the power input port. After brazing, the phase deviations along the section and standing-wave ratio (SWR) were measured. At the operating frequency the SWR was below 1.1. By correcting the shape of some disks with a special tool the SWR was further reduced to 1.02 and simultaneously the band-pass was broadened to $\pm 3 \text{ MHz}$ ($\text{SWR} \leq 1.1$).

In fig.3 the energy gain is plotted as a function of the input power. Also shown is the dynamics of the RF process. We have developed a technique for detection of breakdowns along the section using an acoustic detector.

Fig.4 shows the energy gain and phase shift versus the temperature gradient in the section. As can be seen, the experimental curves are in good agreement with the calculations.

Tests of New Sections

The quasi-constant gradient sections were fabricated by the same technique as the prototype. The section consists of four subsections, each containing 37 cavities, and five coupling cavities between the subsections. To improve the vacuum, approximately in the middle of the section additional evacuation through 16 holes of 4 mm dia. in two cavity cylinders was performed with a magneto-discharge pump. As in the prototype, in the

first quasi-constant gradient section, couplers with an additional evanescent waveguide are used to provide the field symmetry. The tests of the section installed on the 2 GeV linac revealed frequent breakdowns in the input coupler at the RF power from a klystron of 16 MW (the energy gain per section was 56 MeV). The breakdowns in the input diaphragm were detected at much lower fields than in the prototype section. Therefore for subsequent sections an input coupler was designed with a twice as large chamber. The field symmetry was controlled by offsetting the input coupler from the beam axis.

The tests of the coupler at 40 MW proved its sufficient electric strength. (Later the first section with a quasi-constant gradient was extracted from the linac and examined. It was discovered that the breakdown was due to the non-metal inclusions in the input coupler surface. After cleaning, the section was re-installed on the accelerator and since then it has safely operated at various power levels).

The sections with new couplers were also tested on the linac. Fig.5 shows the effect of the RF process and the beam energy gain. The upper power limit at the section input is determined by the dielectric strength of a ceramic window which separates the section from the nitrogen-filled RF channel. During the 2000-h operation on the linac with an average accelerating gradient of 20 MeV/m no degradation in the electric strength has been observed.

Conclusions

New quasi-constant gradient sections provide an accelerating gradient in excess of 20 MeV/m under conventional operating conditions. The problem of suppressing the beam breakup is being investigated experimentally. We have already started fabricating and installing new sections on the 2 GeV linac.

Acknowledgement The authors would like to thank Drs. V.A. Popenko, T.F. Nikitina, Z.M. Kolot, I.N. Gugel' for experimental assistance and Dr. Yu.D. Tur for many useful discussions.

References

1. V.F. Boldyshev, P.I. Gladkikh, V.Yu. Gonchar et al., Trudy XIII Mezhdunarodnoj konferentsii po uskoritelyam chastits vysokikh ehnergij (Novosibirsk, 1986), Nauka Publ., 1987, p.300-303.
2. Z.D. Farkas, H.A. Hogg, G.A. Loew and P.B. Wilson, Proceedings of the 9th International Conference on High Energy Accelerators, Stanford, California, May 1974, p.576.
3. P.B. Wilson, IEEE Trans. Nucl. Sci., NS-28, N 3, p.2742.
4. L.D. Hansborough, W.L. Clark, R.A. Paula et al., 1986 Linear Accelerator Conference Proceedings, Stanford SLAC-Report-303, 1986, p.128-130.

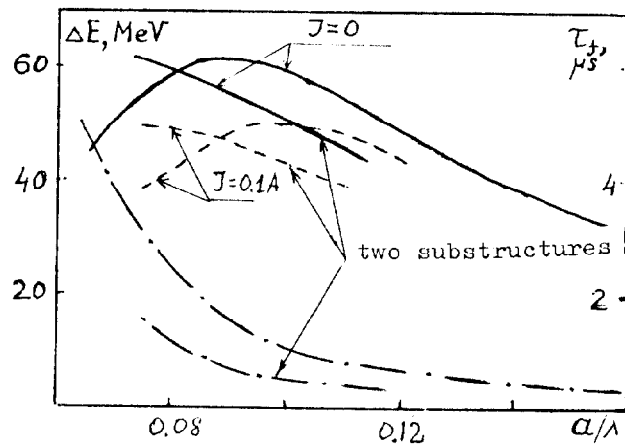


Fig.1 Energy gain ΔE and filling time τ_f vs a/λ ($2a$ is the disk-hole diameter) for two disk-loaded structures.

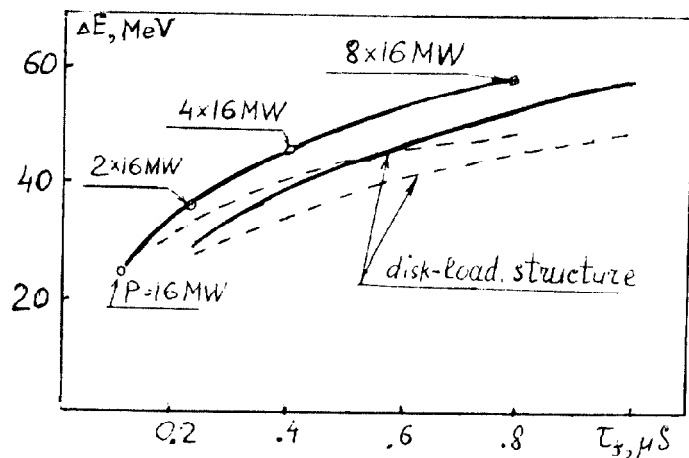


Fig.2 Energy gain ΔE vs filling time for the disk-loaded structure and the "cross-bar" (dashed curves: $J=0.1$ A).

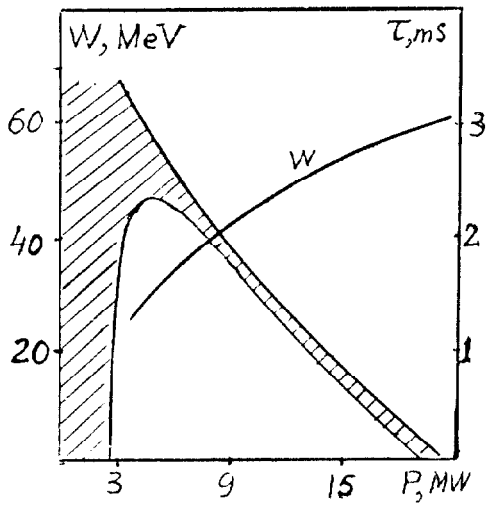


Fig.3 Energy gain and RF breakdown displacement in the constant-impedance structure vs input power for RF-process ($\tau = 0$ at the section end)

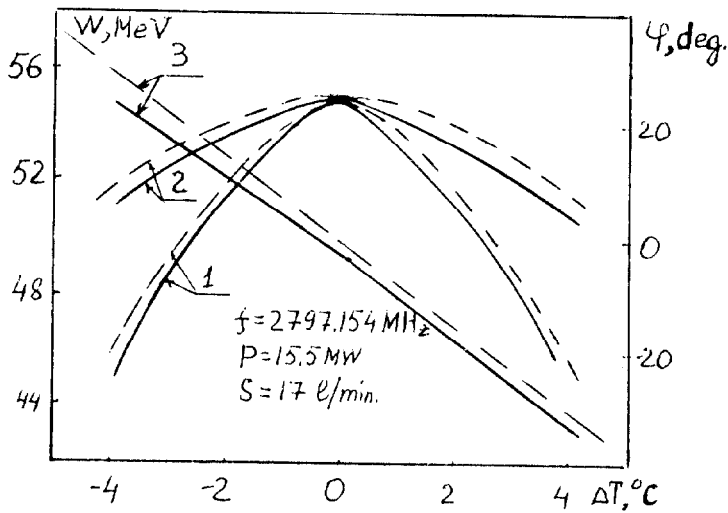


Fig.4 Temperature dependence of the energy gain (1,2) and optimal phase angle between the bunch and the wave crest (3) at the section end. Solid curves: experiment, dashed curves: theory (2): energy gain with optimal phase.

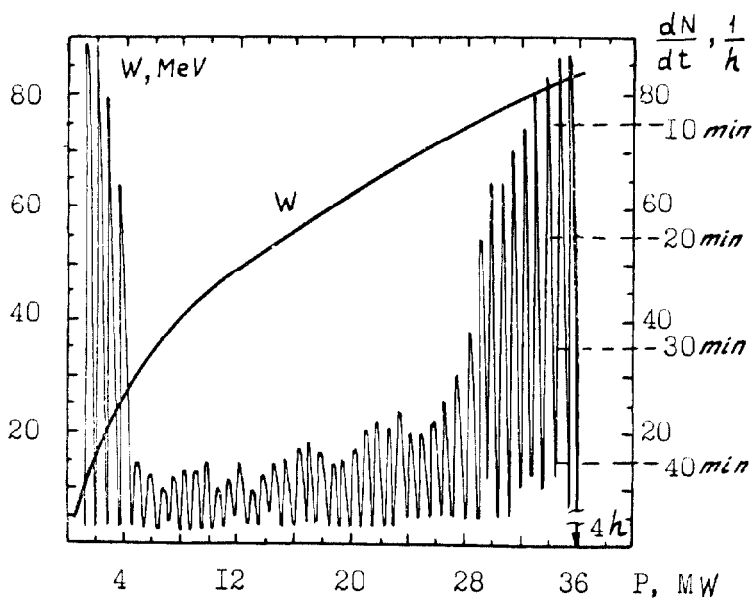


Fig.5 Energy gain for a constant-gradient accelerating section and frequency of RF breakdowns vs input power for RF process.